

High Pressure Route to Magnetic Monopole Dimers in Spin Ice

H. D. Zhou¹, S. T. Bramwell², J. G. Cheng³, C. R. Wiebe^{4,5}, G. Li¹, L. Balicas¹, J. A. Bloxsom², H. J. Silverstein⁵, J. S. Zhou³, J. B. Goodenough³ and J. S. Gardner^{6,7}

1. National High Magnetic Field Laboratory, Florida State University, Tallahassee, FL 32306-3016, USA

2. London Centre for Nanotechnology and Department of Physics and Astronomy, University College London, 17-19 Gordon Street, London, WC1H 0AH, U.K

3. Texas Materials Institute, University of Texas in Austin, Austin, TX 78712, USA

4. Department of Chemistry, University of Winnipeg, Winnipeg, MB, R3B 2E9, Canada

5. Department of Chemistry, University of Manitoba, Winnipeg, MB, R3T 2N2, Canada

6. Indiana University, 2401 Milo B. Sampson Lane, Bloomington, Indiana 47408, USA

7. NIST Center for Neutron Research, NIST, Gaithersburg, MD 20899-6102, USA

The gas of magnetic monopoles in spin ice is governed by one key parameter: the monopole chemical potential. A significant variation of this parameter could access hitherto undiscovered magnetic phenomena arising from monopole correlations, as observed in the analogous electrical Coulomb gas: like monopole dimerisation, critical phase separation, or charge ordering. However, all known spin ices have values of chemical potential imposed by their structure and chemistry that place them deeply within the weakly correlated regime, where none of these interesting phenomena occur. By high pressure synthesis, we have created a new monopole host, $\text{Dy}_2\text{Ge}_2\text{O}_7$, with a radically altered chemical potential that stabilises a large fraction of monopole dimers. The system is found to be ideally described by the classic Debye-Huckel-Bjerrum theory of charge correlations. We thus show how to tune the monopole chemical potential in spin ice and how to access the diverse collective properties of magnetic monopoles.

In the past two decades remarkable technical advances have been made in pressure cell

technology allowing researchers to carry out high pressure investigations in the fields of chemistry, biochemistry, earth and planetary sciences and condensed matter physics. High pressure is used both in the laboratory and on an industrial scale to produce, for example, artificial diamonds, new superconductors and new forms of matter^{1,2}. Pressure is also used to drive materials into new electronic states. Under high pressure, some materials become superconductors, others undergo magnetic phase transitions, and others undergo metal-insulator phase transitions^{3,4}. In magnetic pyrochlore oxides, pressure has been shown to freeze the spin liquid ground state of $\text{Tb}_2\text{Ti}_2\text{O}_7$ ⁵. Pressure is therefore an important weapon in a researcher's arsenal for exploring phase space.

The canonical spin ices, $\text{Ho}_2\text{Ti}_2\text{O}_7$ and $\text{Dy}_2\text{Ti}_2\text{O}_7$, with magnetic Ho or Dy ions⁶⁻⁹, are part of the pyrochlore family of oxides of general formula $\text{A}_2\text{B}_2\text{O}_7$ ¹⁰. They have face centred cubic (fcc) lattice constants of $a_{\text{fcc}} \approx 10.1 \text{ \AA}$. These materials are not very compressible and studies with high physical pressure have not revealed any significant modification of the spin ice properties¹¹. Significantly reduced lattice constants can be obtained in principle by replacing Ti^{4+} with a smaller B ion, such as Ge^{4+} , but it is found that at ambient pressure the pyrochlore structure is only stable if the ratio of the ionic radii, $\rho = r_A/r_B$, is less than 1.55¹⁰. $\text{Dy}_2\text{Ge}_2\text{O}_7$ and $\text{Ho}_2\text{Ge}_2\text{O}_7$, with $\rho \approx 1.8$, adopt a tetragonal structure, when synthesised under ambient pressure¹². The range of stability of the cubic pyrochlore form can be increased using a high pressure, high temperature, synthesis, which extends the regime of stability beyond $\rho = 1.8$ ¹³. The cubic pyrochlore form of $\text{Dy}_2\text{Ge}_2\text{O}_7$ prepared in this way has a lattice constant of 9.9290 \AA , equivalent to a canonical spin ice under enormous physical pressure¹¹.

The microscopic 'dipolar spin ice' Hamiltonian of $\text{Ho}_2\text{Ti}_2\text{O}_7$ and $\text{Dy}_2\text{Ti}_2\text{O}_7$ includes complex dipolar and superexchange interactions^{14,15}. However, to a good approximation, it may be represented by much simpler spin Hamiltonian which is equivalent to the original spin ice model^{6,7}. In this description^{9,14} there are three parameters: the lattice constant a_{fcc} , the rare earth magnetic moment μ and an effective near neighbour exchange parameter J_{eff} . The

equilibrium statistical mechanics then maps onto the statistical mechanics of idealised water ice, such that the low temperature magnetic state is equivalent to the proton disordered state of water ice H_2O ^{6,7}, and shares with it the Pauling configurational entropy⁸. The spin ice state is thus equivalent to pure H_2O , and its excitations are equivalent to the ionic defects H_3O^+ and OH^- ^{6,7,16,17}. The success of this ‘near neighbour spin ice’ description may be attributed to the almost perfect self-screening of the dipole-dipole interaction between rare earth moments in the effective ground state¹⁴.

Although dipole-dipole interactions may be ignored in the spin ice ground state, in Ref.¹⁷ it was shown that inclusion of the dipole-dipole interaction in the excited states causes the ‘ionic defects’ of spin ice to behave as magnetic charges that interact via the magnetic Coulomb law. The description of these defects as magnetic monopoles was firmly established in Ref.¹⁶ by approximating the microscopic spin Hamiltonian $\text{Ho}_2\text{Ti}_2\text{O}_7$ and $\text{Dy}_2\text{Ti}_2\text{O}_7$ to a ‘dumbbell model’, where finite dipoles replace spins. The dumbbell model approximately restores dipolar corrections that are integrated out in the near neighbour description, but still retain three parameters¹⁶. These are the monopole ‘contact distance’, $a = \sqrt{3}a_{\text{fcc}}/4$ (the lattice constant of the diamond lattice inhabited by the monopoles), the elementary monopole charge $Q = 2\mu/a$ ^{16,17} and the monopole ‘self-energy’ ν , which replaces J_{eff} ¹⁶. In Ref.¹⁸ the self energy ν was equated with a monopole chemical potential in the grand canonical ensemble.

The monopole system is a magnetic Coulomb gas of deconfined monopoles and anti-monopoles with overall charge neutrality, which closely approximates a magnetic electrolyte (‘magnetolyte’) in the grand canonical ensemble¹⁸⁻²⁴. Accordingly, experiments on the canonical spin ices reveal strong evidence of the standard field response of such a system, the Wien effect^{19,23,24}, as well as of the applicability of Debye-Hückel theory in zero applied field²¹. In the magnetolyte description of spin ice, the scale of length may be set by the contact distance a and the scale of energy may be set by the Coulomb energy at contact, $\mu_0 Q^2/4\pi a$. Different spin ices - that is, different triplets $\{Q, a, \nu\}$ - should have identical

monopole interaction potentials if energies and lengths are scaled by the above characteristic quantities - so called ‘corresponding states’ behaviour. Thus, the zero-field magnetolyte properties should be fully controlled by the dimensionless temperature T^* ($= 4\pi k_B T a / \mu_0 Q^2$) and the dimensionless monopole density per lattice site x ($\propto c a^3$ where c is the concentration). These two parameters, T^* and x , map out a phase space which, as mentioned above, is expected to be surprisingly rich.

The $x - T^*$ phase behaviour of spin ice has not been determined in detail, but by analogy with electrolyte models²⁵⁻²⁷ we would expect a gradual transition from a weakly correlated magnetolyte at relatively large T^*/x to a strongly correlated magnetolyte at small T^*/x : see Fig. 1. However in a given spin ice, T^* and x cannot be independently varied as x is an explicit function of T^* and the chemical potential ν (see Methods). Thus any one spin ice material maps out a single trajectory in the space of x and T^* , and existing spin ices are found to be firmly in the weakly correlated regime (Fig. 1). In this regime, the fraction of bound monopole-antimonopole pairs is sufficiently small that it may be neglected for most purposes (the field response being an exception: see Ref.²³). Considering, for example, $\text{Dy}_2\text{Ti}_2\text{O}_7$, the chemical potential, ν , is found to be -4.35 K²⁸, which consists (in magnitude) of half the energy required to create a $(+-)$ contact pair, $\epsilon_{\text{pair}}/k_B \approx 5.7$ K, plus half the energy required to unbind the pair, $\mu_0 Q^2 / 4\pi a k_B \approx 3$ K. As the dipole $(+-)$ pair is much higher in energy than the individual $(+)$ or $(-)$ charges, the pairing tendency is weak. In contrast, it can be seen that $\nu \approx 3$ K is the chemical potential that puts monopole-antimonopole pairs or (hetero-)dimers at the same free energy as free monopoles, and thus marks the boundary between the weakly and strongly correlated regimes (see Fig. 1).

The only way to experimentally approach the strongly correlated regime in Fig. 1 is therefore to change the chemical potential ν by changing the energy of pair creation. Fortunately, the latter depends in large part on exchange constants that vary with distance¹⁶. Thus a change of lattice constant from 10.1 Å to 9.93 Å, as achieved by substituting Ti for Ge in $\text{Dy}_2\text{Ti}_2\text{O}_7$ (see Fig. 2), may be sufficient to radically alter the chemical potential. We

have discovered that this is indeed the case, and that $\text{Dy}_2\text{Ge}_2\text{O}_7$, which has a much smaller lattice constant than any spin ice hitherto investigated, lies almost precisely on the boundary of the strongly and weakly correlated regimes in Fig. 1. This means that it has significant monopole dimerisation at all measured temperatures.

It should be noted that the chemical potential and phase behaviour discussed here is not the same as those discussed in Refs.^{16,22} in connection with a field-induced phase transition²⁹. Thus the authors of Ref.¹⁶ argue that the magnetic field in that case favours ordering of positive and negative monopoles on different sublattices, leading to the phase transition, and use the terminology ‘staggered chemical potential’ to describe this. Experimental evidence in support of this scenario is presented in Ref.²². However, the chemical potential we refer to is very different in that it tunes the number density of monopoles without favouring any local ordered arrangement, and is thus equivalent to the chemical potential of ions in an electrolyte (which is not true of the ‘staggered chemical potential’ of Ref.¹⁶).

Results

Pauling Entropy

Phase pure cubic $\text{Dy}_2\text{Ge}_2\text{O}_7$ and $\text{Ho}_2\text{Ge}_2\text{O}_7$ were prepared and characterised as described in the Methods. Here we describe our results in detail for the Dy compound only, and simply note that we have performed a similar characterisation of the Ho compound, which proved to be less interesting in the present context, as it has a more typical chemical potential (see Fig. 1). The magnetic entropy determined by integrating the specific heat divided by temperature (c_m/T) is shown in Fig. 2, where the Pauling residual entropy expected for spin ice⁸ is extremely well reproduced. Magnetometry measurements on $\text{Dy}_2\text{Ge}_2\text{O}_7$ showed this material to have a very similar magnetic moment to $\text{Dy}_2\text{Ti}_2\text{O}_7$. Incurring negligible error, we henceforth assume that the magnetic moment per Dy is equal in the two materials ($9.87 \mu_B$)¹⁵.

Debye-Hückel Theory

In Fig. 3 we show the measured c_m/T plotted against temperature and fitted to Debye-Hückel theory with monopole chemical potential $\nu = (3.35 \pm 0.05)$ K. The method we use has been developed to extend Debye-Hückel theory to a good approximation into the high temperature regime: when applied to $\text{Dy}_2\text{Ti}_2\text{O}_7$ this method gives a similarly good fit to $c_m(T)/T$ with a chemical potential of the expected magnitude. It is based on mapping the system to a lattice gas with site exclusion. The lattice gas is considered to have a temperature-varying chemical potential equal to the sum of the true chemical potential as defined in Ref.²⁸ and the standard Debye-Hückel Coulombic correction to the chemical potential³⁰. Without the latter correction, the predicted specific heat (dotted line in Fig. 3) describes the experimental data well in the limit of high and low temperature, highlighting that this approach is a robust method of deriving an experimental estimate of the monopole chemical potential that is not significantly biased by the limitations of Debye-Hückel theory. In passing, we note that the origin of the approximate collapse of the experimental data and Debye-Hückel calculation onto the ideal lattice gas model at high temperature has a different origin to that at low temperature. In the latter case, the monopole gas is sufficiently dilute that interactions can be neglected, whereas in the former case, a dense and interacting monopole gas reproduces apparent ideal gas behaviour, as the result strong Coulombic screening.

As a further test for consistency we may use our fitted value of ν to derive a value of the effective near neighbour coupling constant, J_{eff} , according to the relationship discussed in Ref.¹⁶, and then compare this with a J_{eff} estimated from the temperature of the specific heat maximum, as discussed in Ref.³¹. The result is $J_{eff} = (0.62 \pm 0.1)$ K, (0.60 ± 0.1) K, respectively, estimates that are equal, within experimental error. For $\text{Dy}_2\text{Ti}_2\text{O}_7$ the corresponding value is $J_{eff} \approx 1.1$ K, which is roughly twice as large. The large difference is accounted for by a more negative (antiferromagnetic) exchange contribution to the spin-spin interaction in $\text{Dy}_2\text{Ge}_2\text{O}_7$ which opposes the positive (ferromagnetic) dipolar coupling, that

is almost the same in the two compounds.

Bjerrum Pairing

The measured chemical potential, -3.35 K, puts $\text{Dy}_2\text{Ge}_2\text{O}_7$ in a regime where monopole dimerisation should be very significant. To confirm this we have used the classic theory of Bjerrum³², who separated the contribution of closely spaced charges out of Debye-Hückel theory and regarded these as distinct chemical entities to be considered alongside the free charges. In Figure 4 we present the energy $u(T)$ of the system found by integrating the specific heat. The result of Debye-Hückel+Bjerrum theory, as described in the Methods, is shown to give an excellent description of the low temperature data, without the addition of any new fitting parameters. This result is not in contradiction with the fit of Fig. 3, as the modified Debye-Hückel theory described in the Methods, including the short distance contribution of charge interactions, naturally incorporates the effect of Bjerrum pairs, to an excellent approximation. The monopoles of $\text{Dy}_2\text{Ge}_2\text{O}_7$ are found to be about 50% dimerised at all measured temperatures.

Discussion

We may put these results in the context of the corresponding states diagram (essentially the phase diagram of T^* versus x) for the restricted primitive model electrolyte, a basic model of electrolyte behaviour. In the case of a continuum electrolyte, there are three significant boundaries on this diagram marking, respectively, the onset of significant dimerisation, the conductance minimum, and phase separation (see, for example, Fig.1 in Ref.²⁵). In $\text{Dy}_2\text{Ge}_2\text{O}_7$ we have reached the first of these boundaries for spin ice. To reach the other boundaries would require us to find a spin ice material with $|\nu| \ll 3.3$ K. However, a lattice Coulomb gas like spin ice may show yet more complex phase behaviour in this limit, including charge ordered phases^{26,27}. In fact the ultimate limit of tuning the monopole chemical potential to $\nu \ll 3$ K has already been identified through numerical studies on the dipolar spin ice model¹⁴. In monopole language, this structure consists of the ordering of ‘double charges’ $\pm 2Q$ to give a magnetic structure with ‘4 spins in/4 spins out’ on alternate tetra-

hedra. This structure (also known as the FeF_3 structure) becomes stable at $\nu = 2.4$ K, $J_{\text{eff}} = 0.2$ K. In the uncharted region between $\nu \approx 3.3$ K and $\nu \approx 2.4$ K we would expect to find a great deal of interesting physics associated with increasing monopole correlations and the gradual appearance of double charges. Our results illustrate that this region should be accessible to experiment, as we have shown how high pressure methods afford the opportunity of dramatically altering the chemical potential of magnetic monopoles in spin ice, to the degree where new aspects of monopole physics can be revealed.

Acknowledgements This work utilized facilities supported in part by the NSF under Agreement No DMR-0944772 and DMR-0654118, and the State of Florida. CRW is grateful for support through the Discovery grant program at NSERC. JSZ and JBG are grateful for financial support from NSF DMR-0904282. LB is supported by DOE-BES through award DE-SC0002613. It is a pleasure to thank PCW Holdsworth and BA Pettitt for numerous useful discussions.

Author Contributions H.D.Z., C.R.W., J.S.G. and S.T.B., conceived the method; J.S.G. and S.T.B. wrote the paper. S.T.B. derived the theory, which was tested by J.B.; H.D.Z. and J.G.C. prepared the samples. H.D.Z., G.L. measures the bulk properties. L.B., C.R.W., J.B.G and J.S.J. contributed to the experimental methodology. H.D.Z. and H.J.S. analysed the crystal structure, H.D.Z., G.L., J.S.G and S.T.B. analysed the heat capacity. All authors contributed to the manuscript.

Author Information Reprints and permissions information is available at npg.nature.com/reprintsandpermissions/. Correspondence and requests for materials should be addressed to J.S.G. (jason.gardner@nist.gov).

Competing Financial Interests The authors declare no competing financial

interests.

Methods

Sample Preparation and Characterisation

Batches of up to 50 milligrams of the pyrochlore dysprosium germanate, $\text{Dy}_2\text{Ge}_2\text{O}_7$, were made in a Walker-type, multi-anvil press. Stoichiometric amounts of Dy_2O_3 and GeO_2 were ground thoroughly, wrapped in gold foil, compressed to 7 GPa and heated to 1000°C. Rietveld refinement of the X-ray powder diffraction pattern confirmed the face-centered cubic space group, (Fd-3m, No. 227) and the absence of any tetragonal pyrogermanate. The room temperature lattice parameter was determined to be 9.9290(5) Å, see Fig. 2 (inset). Temperature and field dependent magnetization measurements confirmed a rare earth magnetic moment of approximately $10 \mu_B$ and a Curie-Weiss constant of 0.0 K. The heat capacity was measured using a thermal relaxation method between 0.34 and 25 K. The lattice contribution was subtracted from the measured specific heat to reveal the magnetic contribution. The energy $u(T)$ was found by numerical integration of the measured specific heat.

Heat Capacity Analysis

To calculate the specific heat the energy per diamond lattice site, u , was written $u = |\nu|x$, where x is the number of monopoles per lattice site: $x = e^{(\nu_{\text{DH}} - |\nu|)/k_B T} (1 + e^{(\nu_{\text{DH}} - |\nu|)/k_B T})^{-1}$. Here ν_{DH} is the standard Debye-Hückel correction to the chemical potential (related to the electrochemical activity coefficient): $|\nu_{\text{DH}}|/k_B T = l_T/(l_D + a)$, where $l_T = \mu_0 Q^2/(8\pi k_B T)$, is the Bjerrum length, $l_D = [2\mu_0 Q^2 x/(k_B T V_d)]^{-1/2}$ is the Debye length, and V_d is the volume per diamond lattice site (for a detailed discussion of these quantities, see Ref.²³). Using these equations x and l_D were determined self consistently, and then the specific heat was found by differentiating u .

To incorporate charge dimers, we considered them as near neighbour pairs, which is appropriate on a lattice²⁶. Their chemical potential is $\nu_d = 2|\nu| - \mu_0 Q^2/(4\pi a)$, giving

the number of pairs per diamond lattice site: $x_B \approx 2 \exp -|\nu_d|/(k_B T)$. The Debye-Hückel correction was modified to avoid double counting these pairs as follows: $\nu_{\text{DH}}/(k_B T) \rightarrow l_T/(l_D + 2a)$. The energy was then calculated as: $u = |\nu_d|x_B + |\nu|x$, which was compared to the measured $u(T)$.

These methods have been comprehensively tested and shown to provide a robust analysis of specific heat data on spin ice materials. They were used to estimate the curves in Fig. 1,3,4. In Fig. 1 the chemical potentials used are: 3.35 K (DyGe), 4.35 K (DyTi), 5.5 K (HoGe) and 5.8 K (HoTi) in an obvious notation: for the Ho materials these are only rough estimates, owing to the difficulty of accurately isolating the electronic specific heat from the nuclear component.⁹

References

1. Solozhenko, V.L. Kurakevych, O.O. Andrault, D. Godec, Y.L. and Mezouar, M. Ultimate Metastable Solubility of Boron in Diamond: Synthesis of Superhard Diamondlike BC₅. *Phys. Rev. Lett.* **102** 015506 (2009).
2. Gregoryanz, E. *et al.* Synthesis and characterization of a binary noble metal nitride. *Nature Materials* **3** 294 (2004).
3. Deemyad, S. and Schilling J.S. Superconducting phase diagram of Li metal in nearly hydrostatic pressures up to 67 GPa. *Phys. Rev. Lett.* **91** 167001 (2003).
4. Gavriluk, A.G. Struzhkin, V.V. Lyubutin, I.S. Ovchinnikov, S.G. Hu, M.Y. and Chow P. Another mechanism for the insulator-metal transition observed in Mott insulators. *Phys. Rev. B* **77** 155112 (2008).
5. Mirebeau, I. Goncharenko, I. N. Cadavez-Pares, P. Bramwell, S. T. Gingras M. J. P. and Gardner, J. S. Pressure-induced crystallization of a spin liquid. *Nature* **420**, 54-57 (2002).
6. Harris, M. J. Bramwell, S. T. McMorrow, D. F. Zeiske T. and Godfrey, K. W. Geometrical frustration in the ferromagnetic pyrochlore Ho₂Ti₂O₇. *Phys. Rev. Lett.*, **79**, 2554-2557 (1997).
7. S. T. Bramwell and M. J. Harris. Frustration in Ising-Type Spin Models on the Pyrochlore Lattice. *J. Phys. Condensed Matter* **10**, L215 - L220 (1998).
8. Ramirez, A. P. Hayashi, A. Cava, R. J. Siddharthan, R. B. and Shastri, S. Zero-point entropy in spin ice. *Nature* **399**, 333-335 (1999).
9. Bramwell, S. T., and Gingras, M. J. P. Spin ice state in frustrated magnetic pyrochlore materials. *Science* **294**, 1495-1501 (2001).

10. Gardner, J. S., Gingras, M. J. P., and Greedan, J. E., Magnetic Pyrochlore Oxides. *Rev. Mod. Phys.* **82**, 53 - 107 (2010).
11. Mirebeau, I. and Goncharenko, I. N., Spin liquid and spin ice under high pressure: a neutron study of $R_2Ti_2O_7$ ($R = Tb, Ho$). *J. Phys.: Condens. Matter* **16**, S653 - S663 (2004).
12. Jana, S., Ghosh, D. and Wanklyn, B.M., Magnetic susceptibility and anisotropy studies of holmium pyrogermanate ($Ho_2Ge_2O_7$) crystal. *J. Mag. Mag. Mat.* **183** 135 - 142 (1998).
13. Troyanchuk, I. O., Preparation and properties of $Er_2V_2O_7$, $Ho_2V_2O_7$, $Y_2V_2O_7$, $Dy_2V_2O_7$ pyrochlore structure. *Inorganic Materials* **26**, 182 - 183 (1990).
14. Melko, R. G., and Gingras, M. J. P. Monte Carlo studies of the dipolar spin ice model. *J. Phys.: Condens. Matter* **16**, R1277-R1319 (2004).
15. Yavorskii, T., Fennell, T., Gingras, M. J. P., and Bramwell, S. T. $Dy_2Ti_2O_7$ Spin Ice: A Test Case for Emergent Clusters in a Frustrated Magnet. *Phys. Rev. Lett.* **101**, 037208 (2008).
16. Castelnovo, C., Moessner, R., and Sondhi, S. L. Magnetic monopoles in spin ice. *Nature* **451**, 42-45 (2008).
17. Ryzhkin, I. A. Magnetic relaxation in rare-earth pyrochlores. *J. Exp. and Theor. Phys* **101**, 481-486 (2005).
18. Jaubert, L. D. C. and Holdsworth, P. C. W. Signature of magnetic monopole and Dirac string dynamics in spin ice. *Nature Phys.* **5**, 258-261 (2009).
19. Bramwell, S. T., Giblin, S. R., Calder, S., Aldus, R., Prabhakaran D., and Fennell, T. Measurement of the charge and current of magnetic monopoles in spin ice. *Nature* **461**, 956-959 (2009).

20. Fennell, T., *et al.* Magnetic Coulomb phase in the spin ice $\text{Ho}_2\text{Ti}_2\text{O}_7$. *Science* **326**, 415-417 (2009).
21. Morris, D. J. P., *et al.* Dirac strings and magnetic monopoles in the spin ice $\text{Dy}_2\text{Ti}_2\text{O}_7$. *Science* **326**, 411-414 (2009).
22. Kadowaki, H., *et al.* Observation of magnetic monopoles in spin ice. *J. Phys. Soc. Jpn.* **78** 103706 (2009).
23. Giblin S. R., Bramwell S. T., Holdsworth P. C. W., Prabhakaran D. and Terry I., Creation and measurement of long-lived magnetic monopole currents in spin ice. *Nature Physics*, **7** 252-258 (2011).
24. Bramwell S. T. Dimensional analysis, spin freezing and magnetization in spin ice. *J. Phys.: Condens. Matter* **23** 112201 (2011).
25. Weingärtner, H. Corresponding states for electrolyte solutions. *Pure. Appl. Chem.* **73** 1733-1748 (2001).
26. Kobelev, V. Kolomeisky, A. B. and Fisher, M. E. Lattice models of ionic systems. *J. Chem. Phys.* **116** 7589 - 7598 (2002).
27. Ciach, A. and Stell, G. Effect of competition between Coulomb and dispersion forces on phase transitions in ionic systems. *J. Chem. Phys.* **114** 3617-3630 (2002).
28. Jaubert L. D. C. and Holdsworth P. C. W. Magnetic monopole dynamics in spin ice. *J. Phys.: Condens. Matter* **23** 164222 (2011).
29. Sakakibara, T., Tayama, T., Hiroi, Z., Matsuhira, K. and Takagi, S. Liquid-gas transition in the spin-ice dysprosium titanate. *Phys. Rev. Lett.* **90**, 207205 (2003).
30. Fowler, R. H. and Guggenheim, E. A., *Statistical Thermodynamics*, Cambridge University Press (1939).

31. Bramwell, S. T., Gingras, M. J. P and Holdsworth, P. C. W., chapter on Spin Ice in *Frustrated Spin Systems*, Ed. H. Diep, World Scientific, 2004.
32. Bjerrum, N, *Kgl. Danske Vid. Selskab, Math. -fys. medd.* **7**, 9, (1926).

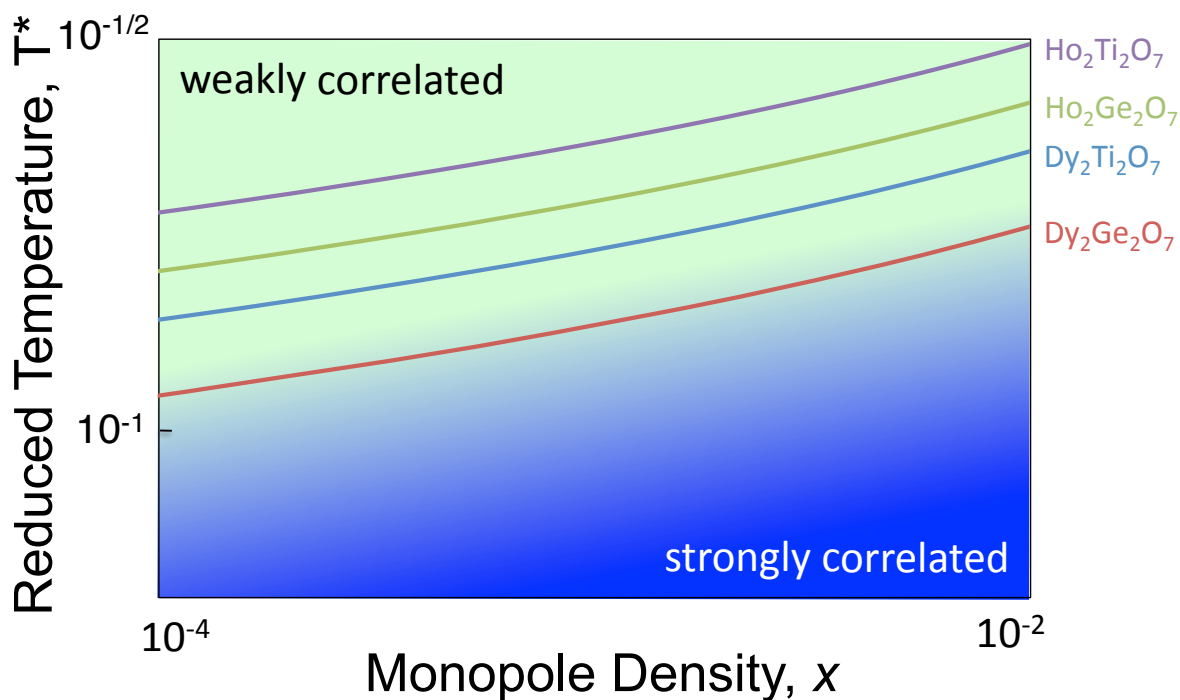


Figure 1: **Creating strongly correlated magnetic monopoles in spin ice.** A corresponding states diagram for spin ice in terms of reduced temperature T^* and monopole density, x . A given spin ice material maps out a single trajectory but the canonical spin ices such as $\text{Dy}_2\text{Ti}_2\text{O}_7$, $\text{Ho}_2\text{Ti}_2\text{O}_7$ lie in the weakly correlated regime (green) rather than in the strongly correlated regime (blue). By high pressure synthesis we have created a new spin ice $\text{Dy}_2\text{Ge}_2\text{O}_7$ that lies on the boundary of strong and weak correlation (red line), and hence has significant monopole dimerisation at all measured temperatures (we have also created $\text{Ho}_2\text{Ge}_2\text{O}_7$ but this lies in the weakly correlated regime). The strongly correlated regime (lower right) has monopole correlations beyond simple pairing, potentially leading to a gas-liquid transition or charge ordering.

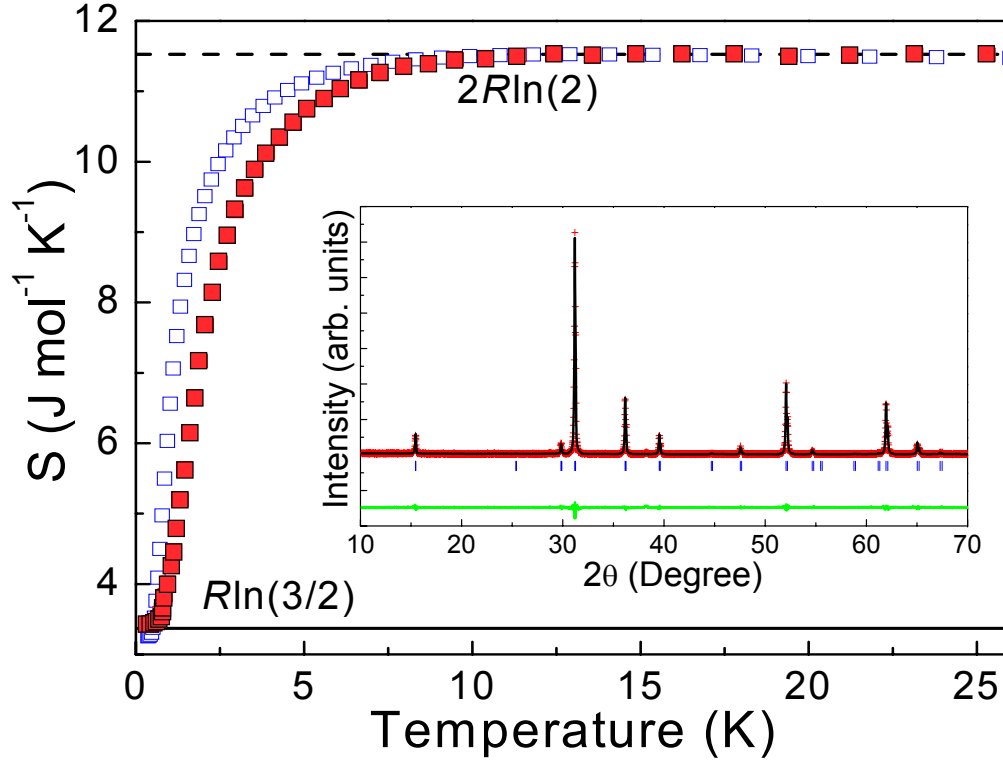


Figure 2: **Proof that $\text{Dy}_2\text{Ge}_2\text{O}_7$ (open) and $\text{Ho}_2\text{Ge}_2\text{O}_7$ (solid) have the characteristic Pauling zero point entropy of spin ice and water ice.** The experimental molar entropy, found by integrating the magnetic specific heat C_m divided by temperature T , when referenced to its high temperature value of $2R \ln(2)$ per diamond lattice site, reveals a zero temperature component of $R \ln(3/2)$ equal to the Pauling value. The inset shows the Rietveld refined x-ray powder diffraction pattern of the cubic pyrochlore phase of $\text{Dy}_2\text{Ge}_2\text{O}_7$ with a lattice parameter of $9.9290(5)$ Å. Errors in the data are smaller than the symbols and represent $\pm 1\sigma$.

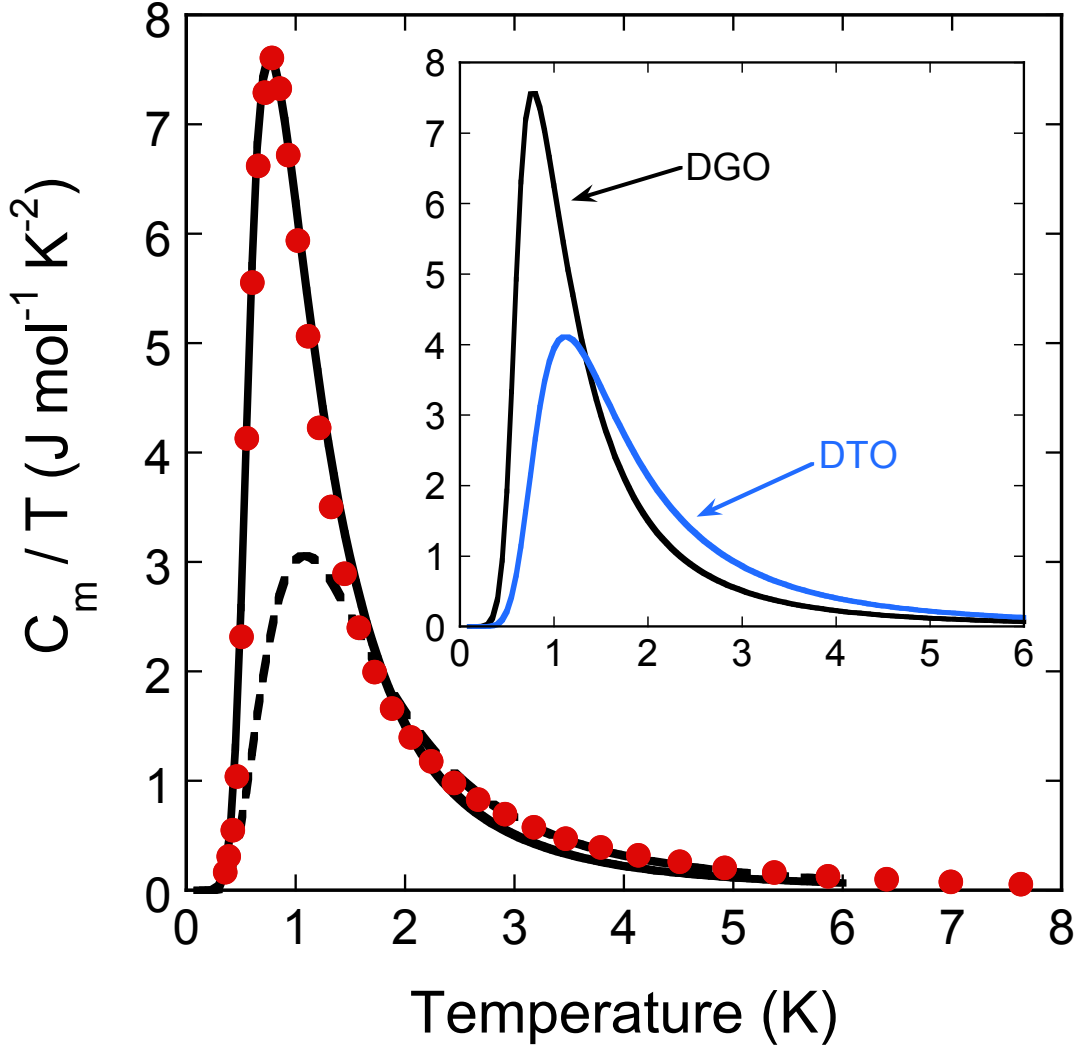


Figure 3: **Measured heat capacity per mole of $\text{Dy}_2\text{Ge}_2\text{O}_7$ at zero field compared to theoretical models.** Main figure: the modified Debye-Hückel theory (Black line), with monopole chemical potential $\nu = 3.35(5)$ K the only adjustable parameter, gives an excellent description of the experimental magnetic heat capacity of $\text{Dy}_2\text{Ge}_2\text{O}_7$ (points). Dashed black line shows the heat capacity of an ideal lattice gas with onsite exclusion with the same chemical potential. This model describes the data well at low temperatures where Coulomb interactions may be neglected, and at high temperatures where the interactions are strongly screened. Inset: the effect of varying chemical potential from -3.35 K (appropriate to $\text{Dy}_2\text{Ge}_2\text{O}_7$ (DGO)) to -4.35 K (appropriate to $\text{Dy}_2\text{Ti}_2\text{O}_7$ (DTO)).

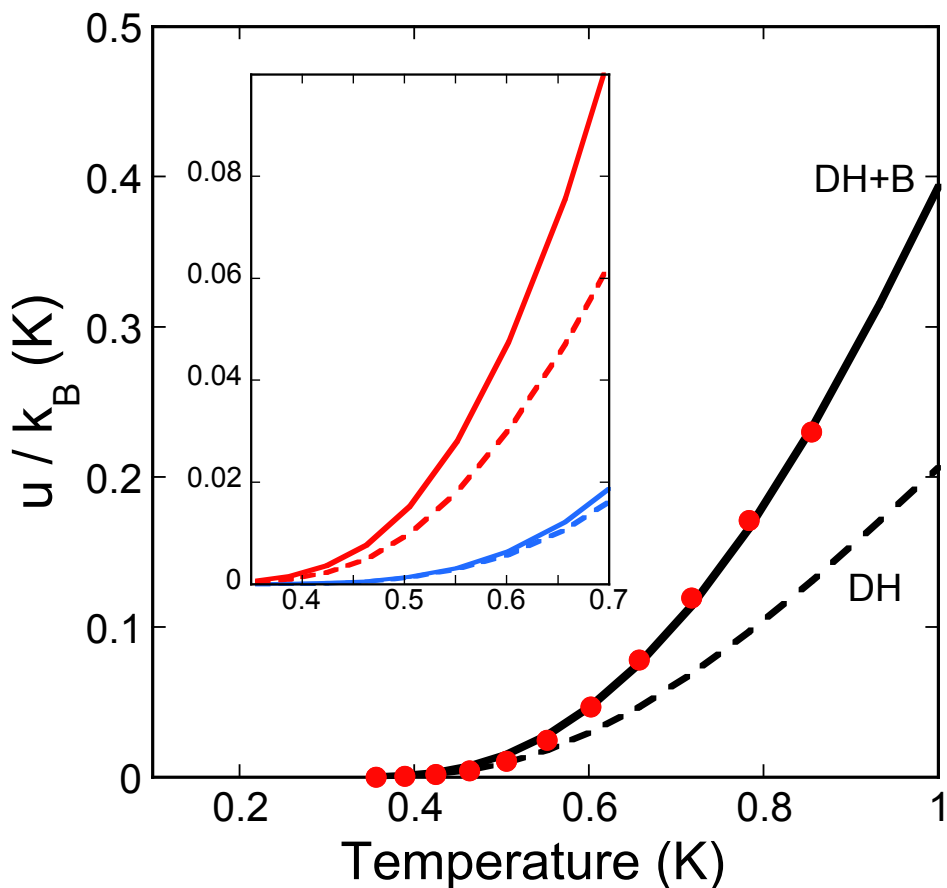


Figure 4: **The experimental energy $u(T)$ of $\text{Dy}_2\text{Ge}_2\text{O}_7$ and the significance of the Bjerrum correction.** Main figure: red circles are experimental data points. Black line is the predicted energy incorporating both free monopoles and $(+-)$ monopole dimers, using the chemical potential estimated from the data of Fig. 3. Black dashed line is the Debye-Hückel theory with a short range cut-off of two lattice spacings, which thus neglects charge dimers. However, our modified Debye-Hückel method fits the data just as well as Bjerrum's method, as it accounts for the dimers to a good approximation (Fig. 3). Inset: upper curve to lower curve are the theoretical energy for $\text{Dy}_2\text{Ge}_2\text{O}_7$ (with and without Bjerrum pairs) and $\text{Dy}_2\text{Ti}_2\text{O}_7$ (with and without Bjerrum pairs) respectively. The Bjerrum correction is much more important for $\text{Dy}_2\text{Ge}_2\text{O}_7$ than for $\text{Dy}_2\text{Ti}_2\text{O}_7$.